Neutron spectroscopic factors of ^{55}Ni hole-states from (p,d) transfer reactions

A. Sanetullaev[1+], M.B. Tsang(曾敏兒)[1*], W.G. Lynch(連致標)[1], Jenny Lee(李曉菁)[1], D. Bazin[1], K.P. Chan[1,2] (陳家鵬), D. Coupland[1], V. Henzl[1], D. Henzlova[1], M. Kilburn[1], A.M. Rogers[1], Z.Y. Sun(孙志宇)[1,3] , M. Youngs[1], R.J. Charity[4], L.G. Sobotka[4], M. Famiano[5], S. Hudan[6], D. Shapira[7], W.A. Peters[7], C. Barbieri[8], M. Hjorth-Jensen[1,9], M. Horoi[10], T. Otsuka[11], T. Suzuki[12], Y. Utsuno[13]

[1]*National Superconducting Cyclotron Laboratory & Department of Physics and Astronomy, Michigan State University, East Lansing, Michigan 48864, USA*
[2]*Physics Department, Hong Kong Chinese University, Shatin, Kong Kong, China*
[3]*Institute of Modern Physics, CAS, Lanzhou 730000, China*
[4]*Department of Chemistry, Washington University, St. Louis, MO 63130, USA*
[5]*Department of Physics, Western Michigan University, Kalamazoo, MI 49008, USA*
[6]*Department of Chemistry, Indiana University, Bloomington, IN 47405, USA*
[7]*Oak Ridge National Laboratory, Oak Ridge, TN 37831, USA*
[8]*Department of Physics, University of Surrey, Guildford GU2 7XH, United Kingdom*
[9]*Department of Physics and Center of Mathematics for Applications, University of Oslo, N-0316 Oslo, Norway*
[10]*Department of Physics, Central Michigan University, Mount Pleasant, MI 48859, USA*
[11]*Department of Physics, University of Tokyo, Tokyo, Japan*
[12]*Department of Physics, Nihon University, Tokyo, Japan*
[13]*Advanced Science Research Center, Japan Atomic Energy Agency, Tokai, Ibaraki 319-1195, Japan*

Abstract

Spectroscopic information has been extracted on the hole-states of ^{55}Ni, the least known of the quartet of nuclei (^{55}Ni, ^{57}Ni, ^{55}Co and ^{57}Co), one neutron away from ^{56}Ni, the N=Z=28 double magic nucleus. Using the ^{1}H(^{56}Ni,d)^{55}Ni transfer reaction in inverse kinematics, neutron spectroscopic factors, spins and parities have been extracted for the $f_{7/2}$, $p_{3/2}$ and the $s_{1/2}$ hole-states of ^{55}Ni. This new data provides a benchmark for large basis calculations that include nucleonic orbits in both the sd and pf shells. State of the art calculations have been performed to reproduce the excitation energies and spectroscopic factors of the $s_{1/2}$ hole state below Fermi energy.

+Present address: TRIUMF, Vancouver, BC Canada
***** Corresponding author: tsang@nscl.msu.edu

Doubly-magic nuclei, with both the proton number (Z) and the neutron number (N) corresponding to closed shells, have played a simplifying role in nuclear structure. Low lying states in somewhat heavier nuclei are often approximated by ignoring the closed shell single particle orbits and considering only the occupied nucleon orbits in higher lying "particle" states in the next major shell. Similarly, low lying states in lighter nuclei are often approximated by considering only unoccupied nucleon orbits ("holes") within the doubly closed shell. In this approximation, effective operators that operate on the particle or hole states provide a means to model changes to the nucleonic wavefunctions in the closed shell "core". This simplification works extremely well in the vicinity of the doubly-magic closed sd shell nucleus ^{40}Ca.

^{56}Ni is the first doubly-magic N=Z nucleus, beyond ^{40}Ca. Produced abundantly in stellar reactions, it plays important roles in many astrophysical processes [1,2]. Despite its importance, its six-day half-life hindered key investigations of ^{56}Ni and its neighbors until radioactive beams became available. Consequently, there are very little data for ^{55}Ni with one neutron less than ^{56}Ni. The only firmly established spin and parity in ^{55}Ni is the ground state with spin and parity of $7/2^-$ [3,4]. Only six out of 22 known states below 7 MeV in this nucleus have tentative spins and parities [3]. Knowing the properties and locations of positive parity excited "hole" states in ^{55}Ni would clarify the energy separations between single particle orbits, which are linked to saturation properties and to the possible role of three-body forces in ab-initio calculations [].

Measurements of hole-states in ^{55}Ni can clarify the extent to which the ^{56}Ni calculations can be regarded as a closed $1f_{7/2}$ core and can also provide the excitation energies of filled $1d_{3/2}$ and $1s_{1/2}$ levels below the Fermi energy. In this paper, we report the first spectroscopic factor measurements of neutron hole states in ^{55}Ni. We find that their successful interpretation requires very large basis calculations involving orbits in both the fp and sd shells. The result may bridge our knowledge gap between the successful interactions for the sd shell and the less successful cousins interactions that describe the pf orbits.

The experiment was performed at the Coupled Cyclotron Facility of Michigan State University. There, a 140 MeV/nucleon primary beam of ^{58}Ni bombarded a 1269 mg/cm^2 beryllium production target. The A1900 fragment separator filtered ^{56}Ni nuclei from the resulting fragmentation products to a purity of 72% and degraded their energies to 37 MeV/nucleon. Details on the identification of the resulting ^{56}Ni beam can be found in Ref [5,6].

This secondary ^{56}Ni beam impinged upon a 9.6 mg/cm^{21}polyethylene $(CH_2)_n$ target. To correct for large size (11mm x 17 mm FWHM) and angular divergence (~1.4°) of this secondary beam, two microchannel plate (MCP) detection systems, 10 cm and 60 cm upstream of target, determined the positions and angles of the incoming projectile on the target [5,6]. The MCP closer to the target monitored the absolute beam intensity throughout the experiment.

Sixteen telescopes of the High Resolution Array, (HiRA) [7], measured the energies and angles of the deuterons and thereby identified the ^{55}Ni states populated by the ^{1}H(^{56}Ni, d)^{55}Ni reaction. These telescopes were located 35 cm from the target where they covered polar angles of 4°- 45° in the laboratory frame. Each telescope contained one 65 μm thick ΔE and a 1500 μm thick E silicon strip detector that were backed by four 3.9 cm thick CsI(Tl) crystals. The 32 horizontal and 32 vertical strips in the E detector effectively subdivided each telescope into 1024 2mm x 2mm pixels, each with an angular resolution of about ±0.16°. The Laser Based Alignment System (LBAS) [8] provided the locations of each pixel relative to the target to an accuracy of 0.3 mm.

The HiRA, MCP and reaction targets were placed in the S800 scattering chamber in front of the S800 spectrometer [9,10], which detected the ^{55}Ni residues. This kinematically complete measurement of deuterons and residues ensures that both particles originate from the ^{1}H(^{56}Ni, d)^{55}Ni reaction. Measurements with a ^{12}C target verified that the ^{12}C nuclei in the polyethene target contributed negligibly to the deuteron cross-sections at the excitation energies of interest to this paper.

The left panel of Fig. 1 shows the 2D spectrum of the laboratory angle vs. laboratory energy of the emitted deuteron in coincidence with ^{55}Ni detected in the S800 focal plane, obtained without benefit of the MCP beam tracking detectors. Two bands corresponding to the ground state of ^{55}Ni and an excited state around 3.18 MeV can be identified. Deuterons with $E_{Lab} <$ 22 MeV stop in the silicon E detector and deuterons 22 MeV < E_{Lab} < 155 MeV stop in the CsI(Tl) crystals. The maximum laboratory angle of the deuterons in this reaction is approximately 32°; there the energy for ground state band increases rapidly with center of mass scattering angle.

The right panel of Fig. 1, shows the improved resolution obtained by correcting the deuteron scattering angle for the position and angle of each beam particle at the target using the MCP beam trackers [6]. At forward angles around 15°, the first excited state of ^{55}Ni at 2.09 MeV can be clearly seen between the stronger bands corresponding to the ground state and the 3.18 MeV excited state at lower and high E_{lab}, respectively. Near the maximum deuteron emission angle of ~30° in the laboratory, (which corresponds to roughly 40° in the center of mass,) the excitation energy resolution worsens due to a number of factors, including target thickness. As cross sections at these larger angles are more sensitive to ambiguities in optical model potentials, we focus on data taken at smaller angles in the laboratory frame.

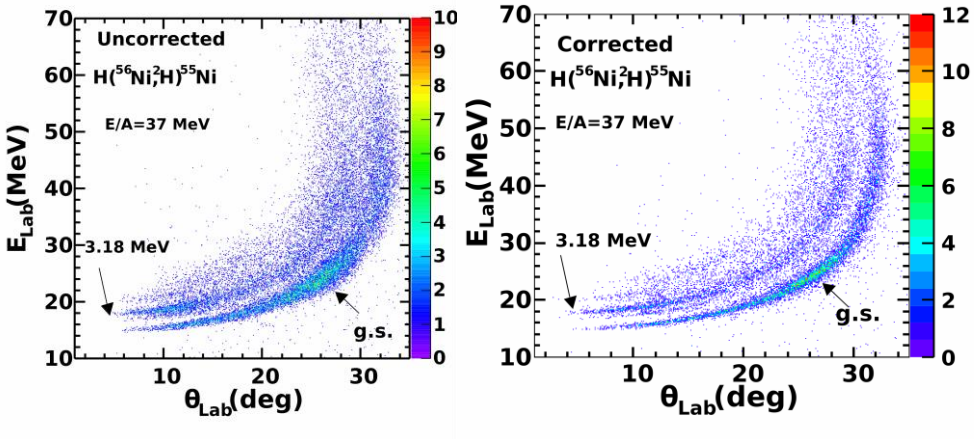

Figure 1: (Color online) Left panel: 2D plot of angle vs. energy for the deuterons detected in the HiRA. Right panel: same as left panel after correcting the beam position and angle using micro-channel plate tracking detectors.

Fig. 2 shows the reconstructed excitation energy of ^{55}Ni at six angles in the center of mass frame. For best resolution, we choose forward angles where the deuteron energy is less than 22 MeV and stops in the Silicon E detectors. Three peaks, corresponding to the ground state, first-excited state at 2.09 MeV, and 3.18 MeV state, can be clearly identified in each angular range in the figure. The energy resolutions of the ground and 3.18 MeV peaks are both about 550 keV. This energy resolution agrees with GEANT4 simulations taking into account the energy and angular straggling in the target and detector resolutions [11]. There is additional yield at excitation energies of approximately 3.75 MeV, but the background at this excitation energy is somewhat uncertain. Unfortunately, deuterons with energy > 22 MeV penetrate the E silicon detectors and enter the CsI(Tl) crystals which has worse resolution. The limitation does not allow the extraction of precise differential cross sections at large angles, θ_{LAB} > 17° for states with high excitation energies greater than 3.5 MeV.

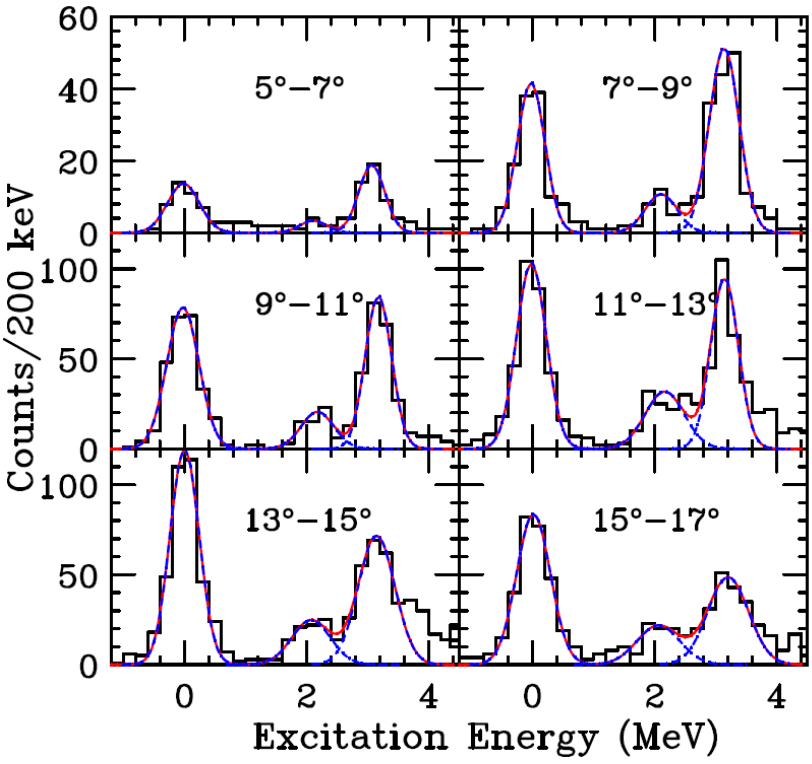

Figure 2: (Color online) Excitation energy of ^{55}Ni constructed from the emitted deuterons in the ^{1}H(^{56}Ni, d)^{55}Ni reaction. Dashed curves are Gaussian fits for individual states and the solid curve is the sum of all the fits.

At the most forward angles, (top left panel), the background is higher due to the close proximity of the telescope to the beam. The total counts detected are lower because of the low geometrical coverage of the HiRA array at these angles. Nonetheless, by using Guassian fits, we are able to extract the counts for all three states identified here in these six angular bins. At larger angles, contributions from the 2.09 MeV state become insignificant.

The angular momentum of the states is extracted from the measured angular distributions shown in Fig. 3. The left panel shows the differential cross-sections for the ground state (solid points) and the first-excited state (open circles). The large separation of the ground-state from the excited-states allows unambiguous extraction of the ground-state peak at all angles. The ground-state angular distribution peaks around 22° with a characteristic shape of l=3 transfer. Using the algorithm developed in ref. [12], we extract the neutron ground state spectroscopic factor of ^{56}Ni(g.s) to be 6.7±0.7, close to the independent particle model value of 8 for a closed $f_{7/2}$ shell. The solid curve is a calculation with the Adiabatic Distorted Wave Approximation (ADWA) [13] using TWOFNR code [14] with the calculated cross section multiplied by 6.7. The calculation describes the shape of the angular distribution reasonably well.

The angular distribution of the weak peak at 2.09 MeV is shown as the open circles in the left panel of Fig. 3. Unlike the ground state, the angular distribution of the 2.09 MeV state peaks around 10° and can be described very well by the angular distributions of a $p_{3/2}$ state. Taking the one-step direct reaction mechanism of the ADWA formalism to be correct implies that the ground state contains a small admixture of a valence neutron in the $1p_{3/2}$ orbit, which lies above the N=28 shell gap. The spectroscopic factor for this state is 0.14±0.03. Such small spectroscopic factor may indicate significant fragmentation of $1f_{7/2}$ and $1p_{3/2}$ strength.

Finally, the angular distribution of the third state at 3.18 MeV is plotted in the right panel of Fig. 3. The differential cross-sections of the first six points are extracted from the Guassian fits shown as dashed curves in Fig. 2. Beyond 19°, the cross-sections

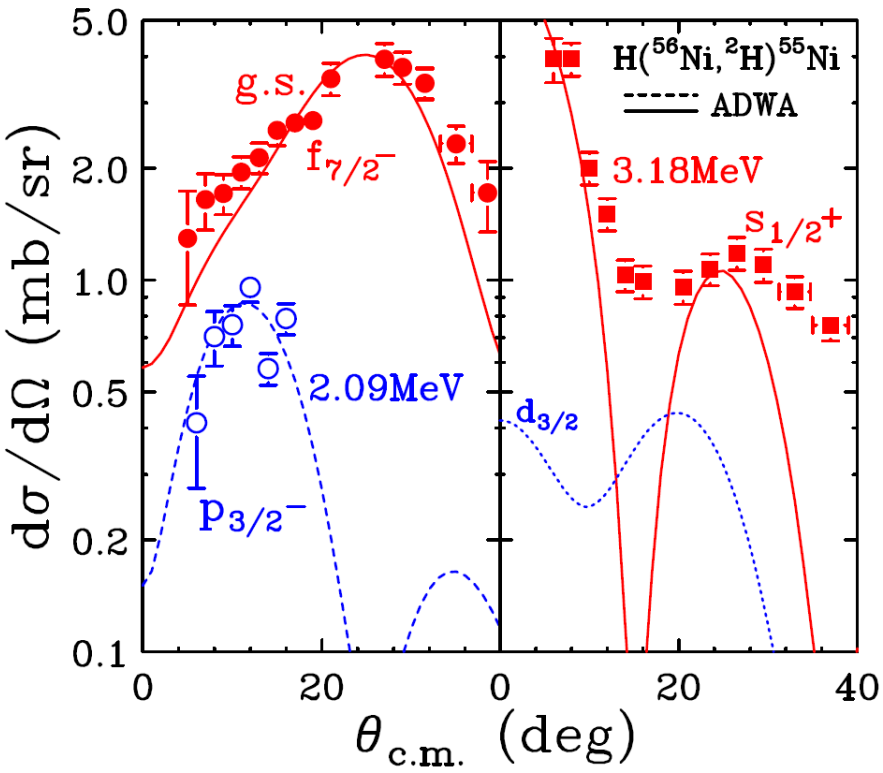

Figure 3: (color online) Deuterons angular distributions for different states of ^{55}Ni. Curves are calculations from ADWA reaction model for individual states as indicated on the figure. Except for the $d_{3/2}$ state which assumes a normalization value of 1, the normalization constants of the other curves yield the spectroscopic values as described in the text.

of the 2.09 MeV state drop to negligible levels and single Guassian fits are sufficient to extract the differential cross-sections. The forward peaking of the angular distribution is consistent with l=0 orbit suggesting that this is the $s_{1/2}$ hole-state below the Fermi-energy in the 1d2s major shell that lies below the $1f_{7/2}$ major shell. The dominance of the $s_{1/2}$ state is evident in Fig. 2 and the existence of such a state is consistent with the systematic of the N=27 isotones [15]. The solid curve is the ADWA calculation assuming ^{1}H(^{56}Ni(g.s), d)^{55}Ni(3.18, $s_{1/2}$) transition consistent with removing a

valence neutron from the $s_{1/2}$ orbit in ^{56}Ni. The extracted spectroscopic factor is 1.0±0.2, exhausting roughly 50% of the total strength expected in the independent particle model.

We observe some excess strength at E*>3.5 MeV. The compilation of levels for the ^{55}Ni nucleus by the National Nuclear Data Center (NNDC) [16] suggests that an excited state at 3.75 MeV could be the $d_{3/2}$ hole state, which could be strongly excited in this transfer reaction. The dotted curve inside the right panel of Fig. 3 represents the calculations of the $d_{3/2}$ state using ADWA model assuming a normalization factor of 1. From Fig. 3, we estimate that the $d_{3/2}$ hole state cross section would be a factor of 5-10 times smaller than that of the $s_{1/2}$ state at $\theta_{LAB}<15°$, roughly consistent with the observed strength. Unfortunately, at larger angles where the $d_{3/2}$ state should have a larger cross section, the deuterons punch into the CsI(Tl) detectors and both the energy and kinematic angular resolution is not good enough to make definitive conclusions.

The shell-model excitation energies and spectroscopic factors for the $f_{7/2}$ and $p_{3/2}$ states, can be calculated relatively accurately in the pf valence space using the standard GXPF1A interaction [17,18]. To describe the energy and spectroscopic factor for the $s_{1/2}$ states, however, requires a valence space that mixes relevant sd orbitals with pf orbitals. Table I shows results from a modified version [19] of SDPFM [20] that freezes the $d_{5/2}$ orbital in the core, and adjusts the single particles energies and the sd-pf monopoles to describe the low-lying states in ^{55}Ni. The results shown by the columns labels "SM1" in Table I predict the properties of deep-hole states in the sd orbit below the Fermi surface reasonably well.

Alternately, one can activate all the sd and pf orbits as valence shells but truncate many-body states appropriately. Specifically, one can assume $1/2^+_1$ and $3/2^+_1$ to be dominantly one-hole states, and limit the number of nucleons excited from the sd shell to the pf shell to one. In addition, one can restrict the number of nucleons in the upper pf orbits ($p_{3/2}$, $f_{5/2}$ and $p_{1/2}$) to be equal to or less than six. To test this truncation, the SDPF-MU interaction [21] was used without

any modifications. This provided reasonable agreement with experimental energy levels and the spectroscopic factors, as shown by columns labeled "SM2" in Table I.

State	E*_expt (MeV)	E*_SM1 (MeV)	E*_SM2 (MeV)	E*_SCGF (MeV)	SF_expt	SF_SM1	SF_SM2	SF_SCGF
$f_{7/2}$	0	0	0	0	6.7±0.7	6.75	6.94	5.78
$p_{3/2}$	2.09	1.895	2.281	4.34	0.19±0.03	0.189	0.13	0.06
$s_{1/2}$	3.18	3.039	3.755	11.48	1.0±0.2	1.57	1.21	1.10
$d_{3/2}$	(3.752)	4.453	4.453	12.47	NA	2.88	1.68	2.16

Table I: Experimental and calculated information on the $f_{7/2}$, $p_{3/2}$ and $s_{1/2}$ states. The notation of "SM1" , "SM2", and "SCGF" refers to the shell-model calculations using a modified SDPFM interaction, those with the SDPF-MU interaction, and those with self-consistent Green's functions theory respectively.

Calculations were also performed with ab-initio self-consistent Green's functions (SCGF) theory [22], which can estimate separation energies and spectroscopic factors of main quasi-hole peaks away from the major valence shell. One calculation based on the two-body chiral N3LO interaction puts the $p_{3/2}$ state at 4.3 MeV with a weak spectroscopic factor [23]. However, the $s_{1/2}$ and $d_{3/2}$ states are predicted to be deeply bound corresponding to excitation energies around 12 MeV rather than the observed values. Together with the main peak, which is labeled as "SCGF" in Table I, there are also other satellite peaks spread between 11 and 18 MeV. The overestimated excitation energies of all the sd states is an artifact due to the missing three-body forces in the Hamiltonian. These are now known to correct the energy separation between the pf and sd shells by several MeV [23,24]. The spectroscopic factors predicted by SCGF appear in rather good agreement with the observation.

Summary and Conclusion

In the present work, the deuteron cross-sections are extracted from a kinematically-complete experiment ^{1}H(^{56}Ni, d)^{55}Ni using a high resolution array, micro channel plate tracking detectors and

the S800 spectrometer. The good angular and energy resolution of the data allows us to extract the spectroscopic information for three low-lying states of ^{55}Ni. This data provides a bench-mark for calculations that include levels in both the 2s1d and 1f2p shells. Unlike the case for hole states in ^{39}Ca made by removing one neutron from doubly closed shell ^{40}Ca, the description of the low lying structure of ^{55}Ni requires a model space that spans both the sd and fp major shells. The state-of-the-art shell model calculations reproduce the excitation energies and spectroscopic factors reasonably well. Self-consistent Green's functions theory, on the other hand reproduces the spectroscopic factors, but not the excitation energy of the $s_{1/2}$ state, a discrepancy that may reflect the neglect of 3 body forces in these calculations.

Acknowledgements:

The authors would like to thank Professor B.A. Brown for stimulating discussions and Professor J. Tostevin for the use of the programs TWOFNR. This work is supported by the National Science Foundation under Grant No. PHY-0606007. M.H. acknowledges U.S. NSF Grant No. PHY-1068217.

References:

[1] M.B. Aufderheide, G.E. Brown, T.T.S. Kuo, D.B. Stout, P. Vogel, Astrophys. J. **362**, 241 (1990).
[2] R. K. Wallace and S. E. Woosley, Astrophys. J., Suppl. Ser. **45**, 389 (1981).
[3] Huo Junde, Nuclear Data Sheets, **109**, 787 (2008).
[4] D. Mueller, E. Kashy, and W. Benenson, Phys. Rev. C **15**, 1282 (1977).
[5] A. Rogers, PhD thesis, Michigan State University (2009).
[6] A. Sanetullaev, PhD thesis, Michigan State University (2011).
[7] M.S. Wallace et al., Nucl. Instrum. Methods Phys. Res. A**583**, 302 (2007).
[8] A.M. Rogers et al., Nucl. Instr. and Meth. A **707** (2013) 64.
[9] J. Yurkon et al., Nucl. Instrum. Methods Phys. Res. A **422**, 291 (1999).
[10] D. Bazin et al., Nucl. Instrum. Methods Phys. Res. B **204**, 629 (2003).
[11] J. Lee, PhD thesis, Michigan State University (2010).

[12] Jenny Lee, M.B. Tsang, W. G. Lynch, Phys. Rev. C **75**, 064320 (2007).
[13] R.C. Johnson and P.J.R. Soper, Phys. Rev. C**1**, 976 (1970).
[14] M. Igarashi et al., Computer Program TWOFNR (Surrey University version).
[15] F. Lu et al., accepted by Phys. Rev. C (2013).
[16] National Nuclear Data Center, http://www.nndc.bnl.gov/
[17] M. Honma, T. Otsuka, B.A. Brown, and T. Mizusaki, Phys. Rev. C, **79**, 034335 (2004).
[18] M. Honma, T. Otsuka, B.A. Brown, and T. Mizusaki, Eur, Phys, J. A **25**, Suppl.1, 499 (2005).
[19] Y. Utsuno, T. Otsuka, T. Mizusaki, and M. Honma, Phys. Rev. C **60**, 054315 (1999).
[20] E.S. Diffenderfer et al, Phys. Rev. C **85**, 034311 (2012).
[21] Y. Utsuno, T. Otsuka, B. A. Brown, M. Honma, T. Mizusaki, and N. Shimizu, Phys.Rev. C **86**, 051301(R) (2012).
[22] C. Barbieri, M. Hjorth-Jensen, Phys. Rev. C **79**, 064313 (2009).
[23] A. Cipollone, C. Barbieri, and P. Navrátil, Phys. Rev. Lett. **111**, 062501 (2013).
[24] C. Barbieri et al., to be published.